Effect of root spacing on interpretation of blade penetration tests-full-scale physical modelling

Meijer, G. J.; Knappett, J. A.; Bengough, A. G.; Loades, K. W.; Nicoll, B. C.

Published in:
Physical Modelling in Geotechnics

DOI:
10.1201/9780429438660-60

Publication date:
2018

Document Version
Peer reviewed version

Author Accepted Manuscript version of Meijer, GJ, Knappett, JA, Bengough, AG, Loades, KW & Nicoll, BC 2018, Effect of root spacing on interpretation of blade penetration tests-full-scale physical modelling. in A McNamara, S Divall, R Goodey, N Taylor, S Stallebrass & J Panchal (eds), Physical Modelling in Geotechnics: Proceedings of the 9th International Conference on Physical Modelling in Geotechnics (ICPMG 2018), July 17-20, 2018, London, United Kingdom. vol. 1, CRC Press/Balkema, pp. 425-430, 9th International Conference on Physical Modelling in Geotechnics, ICPMG 2018, London, United Kingdom, 17/07/18. https://doi.org/10.1201/9780429438660-60

Effect of root spacing on interpretation of blade penetration tests – full-scale physical modelling

G. J. Meijer & J. A. Knappett
University of Dundee, Division of Civil Engineering, Dundee DD1 4HN, UK

A. G. Bengough
University of Dundee, Division of Civil Engineering, Dundee DD1 4HN, UK
James Hutton Institute, Invergowrie, Dundee DD2 5DA, UK

K. W. Loades
James Hutton Institute, Invergowrie, Dundee DD2 5DA, UK

B. C. Nicoll
Forest Research, Northern Research Station, Roslin, Midlothian EH25 9SY, UK

ABSTRACT: The spatial distribution of plant roots is an important parameter when the stability of vegetated slopes is to be assessed. Previous studies in both laboratory and field conditions have shown that a penetrometer adapted with a blade-shaped tip can be used to detect roots from sudden drops in penetrometer resistance. Such drops can be related to root properties including diameter, stiffness and strength using simple Winkler foundation models, thereby providing a field instrument for rapid quantification of root properties and distribution. While this approach has proved useful for measuring single widely-spaced roots, it has not previously been determined how the penetrometer response changes as a result of roots being in close proximity. Therefore in this study 1-g physical modelling (at 1:1 scale) was conducted to study the effect of vertical root spacing using horizontal, straight 3D-printed root analogues. Results show that when roots are closely spaced, there is significant interaction between them, resulting in higher apparent root displacements to failure and an increased amount of energy being dissipated. This preliminary work shows that the interpretive models used to analyse the penetrometer trace require further development to account for root-soil-root interactions in densely rooted soil.

1 INTRODUCTION

Plant roots can reinforce soil through mechanical action (similar to fibre-reinforced soil) and hydrological effects (by reducing the soil water content and increasing soil matric suction through water uptake by the plant) (e.g. Coppin and Richards 1990). To make quantitative predictions for either of these effects, the spatial distribution of roots is an important parameter. It is however difficult to obtain this information without time-consuming root sampling techniques.

To address this problem, Meijer et al. (2016) proposed new field measurement techniques. One of these, the so-called 'blade penetrometer', can be used to infer root depths and root properties from the penetrometer depth–resistance curve. The penetrometer tip shape was enhanced with a thin blade. This greatly increases the chance a root will be hit per unit of tip area, making the penetrometer more sensitive to identifying roots (Meijer et al. 2016). Roots will be visible in the depth–resistance trace as peaks: from the moment a root is hit the penetrometer resistance will increase, up to the point at which the root fails, visible as a sudden decrease in penetrometer resistance (Figure 1). Interpretative methods were developed to infer root properties such as root diameter from the characteristics of these root reinforcement peaks, based on the assumption that the root either fails in pure bending or pure tension. These properties can then in turn be used to calculate mechanical root-reinforcement using existing models.

This methodology was successfully tested in the laboratory using dry sand and 3-D printed Acrylonitrile Butadiene Styrene (ABS) root analogues (Meijer et al. 2017a). It was shown that for these root analogues the model based on root failure in bending

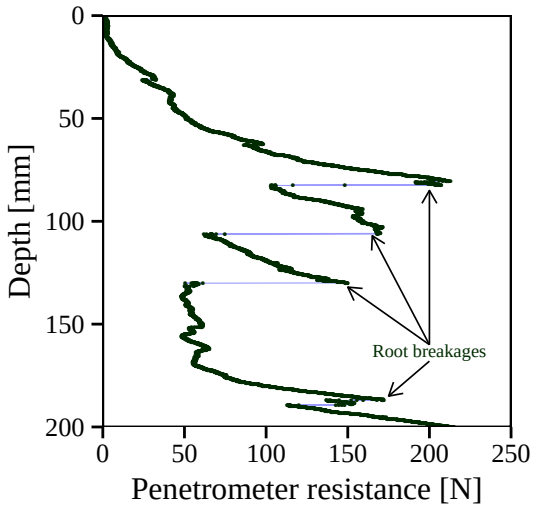

Figure 1: Field depth–penetrometer resistance trace measured in a clayey silt soil rooted with oak trees (Meijer et al. 2017b). Depth and resistance were sampled at 100 Hz (measurement points in green).

worked best. The best predictions were made using the magnitude of the sudden decrease in penetrometer resistance associated with root analogue failure, rather than the displacement required to reach failure. Testing in real soils with live vegetation confirmed these results (Figure 1), although for thinner roots an interpretative model based on root failure in tension worked better (Meijer et al. 2017b).

The laboratory investigations by Meijer et al. (2017a) only considered individual roots. In reality however roots may be closely spaced. When the displacement required to reach root failure is larger than the root spacing, multiple roots might be loaded by the penetrometer at the same time, making interpretation of the results much more difficult. Furthermore, root–soil–root interaction might occur.

To investigate these effects, a preliminary physical modelling study was performed using ABS root analogues in dry medium dense and dense sand investigating the effect of closely spaced roots on the penetrometer depth–resistance response.

2 METHODS

2.1 *Laboratory experiments*

A series of blade penetrometer tests was performed in the laboratory, using closely spaced root analogues in dry sand. All tests were performed at 1-g at a 1:1 scale. To ensure accurate scaling, the following conditions should match the conditions in typical field conditions:

1. Root mechanical properties
2. Root diameter, length and spacing
3. Soil stress level

Similar to Meijer et al. (2017a), Acrylonitrile Butadiene Styrene (ABS) plastic was used as root ana-

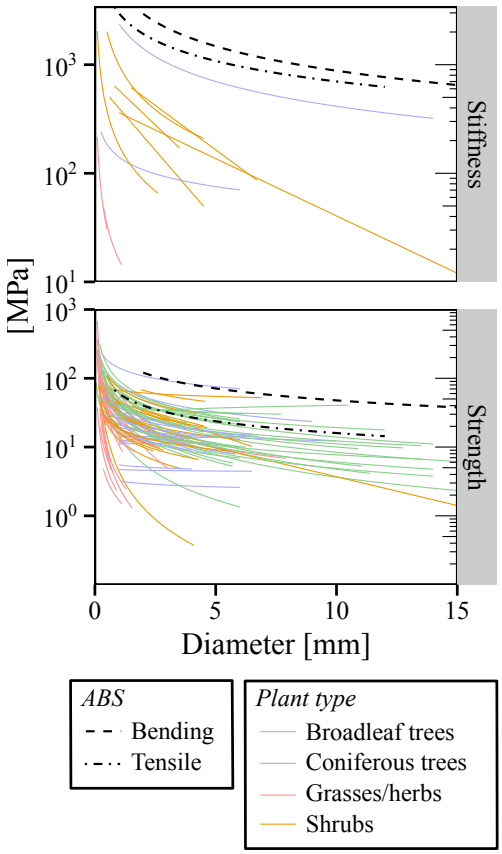

Figure 2: ABS tensile and bending properties compared to tensile strength and Young's modulus for real plant roots reported in the literature (see Meijer (2016) for sources). The ABS stiffness is plotted as the secant stiffness at 90% strength.

logue material. This material has comparable mechanical characteristics to plant roots (Liang et al. 2015, Meijer et al. 2016), see Figure 2. The bending strength and stiffness has been measured in 3-point bending (Meijer et al. 2017a). Peak strength and stiffness reduces with increasing diameter. This is fitted using the following curve:

$$\sigma_b = \alpha_\sigma \left(\frac{d}{d_{ref}} \right)^{\beta_\sigma} \tag{1}$$

where σ_b is the peak bending strength, d the diameter and $d_{ref} = 1$ mm a reference diameter. $\alpha_{\sigma,b} = 180$ MPa and $\beta_{\sigma,b} = -0.577$. A similar relation was used for the bending stiffness E_b:

$$E_b = \alpha_E \left(\frac{d}{d_{ref}} \right)^{\beta_E} \tag{2}$$

where $\alpha_{E,b} = 4937$ MPa and $\beta_{E,b} = -0.749$. Stiffness E_b is defined as the secant stiffness at 90% strength rather then the Young's modulus, as it gives a better approximation of the non-linear stress–strain curve when a linear elastic material model is used in the interpretation (Meijer et al. 2017a).

The soil material used was dry Congleton silica sand (HST95) with relative densities of $I_d = 50\%$ (medium dense) or $I_d = 80\%$ (dense). The critical state friction angle is $\phi_{cv} = 32°$ and peak friction angles are $\phi' = 39°$ and $\phi' = 45°$ respectively. Dry

Figure 3: Box prior to pluviation

unit weight γ' was 16.0 and 16.9 kNm^{-3} respectively (Lauder 2010).

Root analogues were printed in segments of 200 mm using a rapid prototyper ('3D-printer'). Root analogue diameters were 2 or 4 mm. The tested root length was $L = 400$ mm, obtained by gluing together two root analogue segments using epoxy resin and a printed ABS coupler with a length of 15 mm and an external diameter 3 mm larger than that of the analogue. The root analogue diameters tested are near the commonly used threshold between 'thin' and 'thick' roots of $d = 2$ mm (e.g. Achat et al. 2008), making them representative of an 'average' root. The root length is on the short end of the root length/root diameter ratio compared to values measured for Norway spruce roots (Giadrossich et al. 2013):

$$L = 390d^{0.56} \tag{3}$$

A plastic box lined with 10 mm thick adhered wooden panels with internal dimensions 530× 330 × 310 mm (length × width× height) was used. Prior to sand pluviation, roots were glued into pre-drilled holes in the wooden panel. Roots were suspended by wires (cut prior to commencing a test) to prevent significant deformations due to self-weight (Figure 3).

For every test, two horizontal root analogues were used. The first root analogue was located at $z = 150$ mm below the soil surface and the second analogue at a distance of $3d$ below this. (centre-to-centre spacing $s/d = 3$). These depths correspond with typical rooting depths in the field were most roots grow near the surface because of availability of water, oxygen and nutrients. Typically, over 50% of plant roots can be found in the top 300 mm of the soil (Jackson et al. 1996). Effective soil stresses in experiments are therefore representative of those found in the field (assuming suction levels are small). The adopted root spacing can be expressed in terms of root area ratio (RAR, i.e. the percentage of soil cross-sectional area covered by root):

$$RAR \approx \frac{\frac{\pi}{4}d^2}{ws} \tag{4}$$

where $w = 30$ mm is the width of the penetrometer. For $d = 2$ mm root analogues, $RAR = 1.75\%$ while

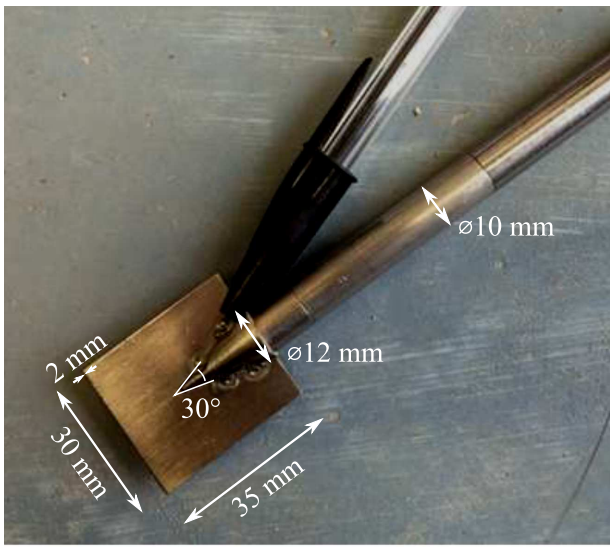

Figure 4: Blade penetrometer. Ballpoint pen for scale.

for $d = 4$ mm $RAR = 3.49\%$, which is high compared to the field where typically $RAR < 1\%$ (e.g. Bischetti et al. 2005. Field values are however average values, so locally RAR might be higher. Thus, $s/d = 3$ can be seen as an upper limit for realistic root spacing.

Subsequent to root placement the box was filled with dry sand to a height of 300 mm using a slot pluviator. Multiple penetrometer tests were conducted per box. The lateral spacing between roots was at least 65 mm ($s/d > 16$) to minimise interaction between tests.

2.2 *Equipment and test programme*

The blade penetrometer was constructed by welding a blade to a standard agricultural penetrometer (⌀12 mm, 30° tip). The shaft was thinner (⌀10 mm) to minimise shaft friction (Figure 4).

Tests were performed using a universal testing machine (Instron 5980). The extension rate was 300 mm min^{-1}, similar to Meijer et al. (2016). Both force and displacement were logged at 20 Hz.

Roots were loaded by the penetrometer at a distance of 300 mm from the point where the root was anchored in the side of the box. Tests were performed using both root diameters (2 and 4 mm) and both soil densities (50% and 80%), totalling 4 tests.

Additional blade penetrometer tests were performed in areas of the container that contained no roots. The results of these 'fallow' tests were subtracted from the results of the rooted test to find the contribution of the root analogues to penetrometer resistance.

Root reinforcements measured in rooted tests were compared to the results obtained for single roots as measured by Meijer et al. (2017a).

2.3 *Interpretative methods*

Meijer et al. (2017a) derived an interpretative method for roots loaded in bending by a penetrometer based on Euler-Bernoulli beam theory. The maximum force

a root can sustain before breaking in bending when loaded perpendicularly by a penetrometer (F_u) can be estimated by:

$$F_u = \xi_F d^2 \sigma_b^{0.5} p_u^{0.5} \quad (5)$$

where $\xi_F = 1.02$, d is the root diameter [mm], σ_b the maximum root strength in bending [MPa] and p_u the soil resistance against lateral root displacement [MPa]. The latter is expressed as $p_u = p/d$, where p is the maximum mobilised lateral soil resistance according to p-y theory (e.g. Reese and Van Impe 2011). The corresponding lateral root displacement to failure u_u is given by:

$$u_u = \xi_u d \sigma_b^2 E_b^{-1} p_u^{-1} \quad (6)$$

where $\xi_u = 0.098$ and E_b is the root stiffness in bending. The force-displacement behaviour is given by:

$$F(u) = \xi_F \xi_u^{-0.25} u^{0.25} d^{1.75} E_b^{0.25} p_u^{0.75} \quad (7)$$

Integrating Equation 7 between $u = 0$ and $u = u_u$ gives the total amount of work (W_u) dissipated by the root before failure occurs:

$$W_u = 0.8 \xi_F \xi_u d^3 \sigma_b^{2.5} E_b^{-1} p_u^{-0.5} \quad (8)$$

Equations 5–8 can also be used for roots reinforcing soil in direct shear. When they cross the shear plane perpendicularly, $\xi_F = 0.89$ and $\xi_u = 1.05$. Thus the results from a blade penetrometer test can be directly used to estimate the root behaviour in direct shear loading.

p was estimated using a p-y model for piles in dry sand, ignoring surface wedge formation near the surface (Reese and Van Impe 2011):

$$p = A_s d z \gamma' \left[K_a \left(\tan^8 \beta - 1 \right) + K_0 \tan \phi' \tan^4 \beta \right] \quad (9)$$

where z is the depth, $K_a = 0.4$ and $K_0 = 1 - \sin \phi'$ coefficients of lateral earth pressure, A_s a dimensionless model constant and $\beta = 45° + \phi'/2$. It can be readily seen from Equations 5–8 that the behaviour of the root does not only depend on root properties but also on the soil resistance. At $z = 150$ mm depth, $p_u \approx 0.19$ ($I_d = 50\%$) or $p_u \approx 0.47$ MPa ($I_d = 80\%$).

3 RESULTS

The penetrometer force–displacement behaviour proved difficult to interpret, mainly due to post-failure root analogue effects. After root failure, during subsequent penetrometer displacement both broken ends might have got stuck on the shoulder of the cone, causing additional peaks and troughs in the trace. When dealing with multiple roots, the behaviour of subsequently loaded roots got obscured by these artefacts. To address this problem, sudden drops in force that corresponded with root analogue failure were identified by audio observations. Failure coincided with a clear 'snapping' noise.

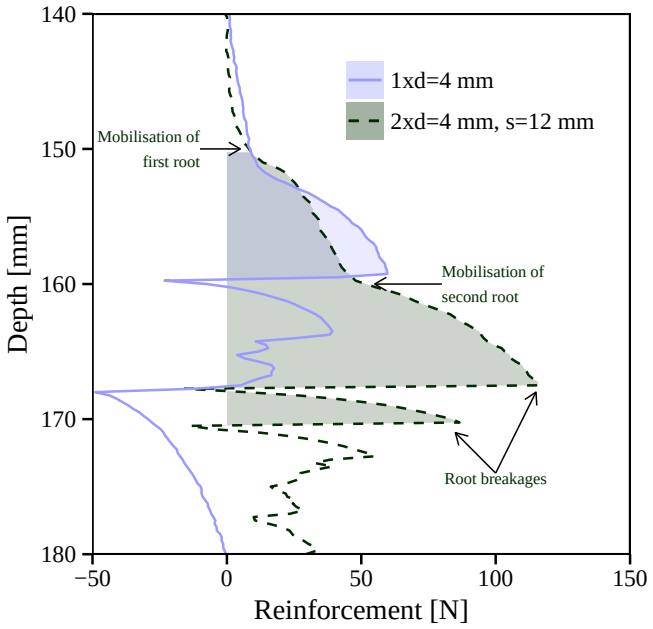

Figure 5: Root reinforcement traces for a single and two $d = 4$ mm roots in $I_d = 50\%$ sand. 's' is root centre-to-centre distance. Shaded areas indicate root action.

The depth–root reinforcement traces are shown in Figures 5–8, both for tests with two closely spaced roots and tests containing only a single root at $z \approx 150$ mm. Both the experimental and model results for single roots shows an increase in F_u with diameter and soil relative density. In contrast, u_u increases with diameter but is inversely correlated to relative density. The only exception is the $d = 2$ mm root analogue in dense soil, for which u_u is much larger than expected compared to other tests.

Increasing the relative density has a distinct effect on the effect of closely spaced $d = 4$ mm root analogues (Figure 6). In the $I_d = 80\%$ case $s \approx 2$–$3u_u$, resulting in what appears to be independent behaviour of the two analogues. When $I_d = 50\%$ however, $s \approx u_u$, resulting in interaction between the two root analogues (Figure 5). The upper root analogue in this case displaced much further before reaching failure compared to a test containing only a single analogue. Similar interaction effects were observed for two $d = 2$ mm roots in $I_d = 50\%$ (Figure 7) or $I_d = 80\%$ sand (Figure 8). Breakage of both roots occurred almost at similar depths and at much larger displacements compared to tests on a single root.

The total amount of work dissipated by two closely spaced roots is higher then the sum of two individual roots. This effect is more pronounced for thinner roots and in soil with lower relative densities (Table 1).

4 DISCUSSION

Since root properties σ_b and E_b are constant, according to Equation 8 only a decrease in p_u can explain

Table 1: Summary of experimental results.

Diameter	I_d	Measured				Predicted/Measured			f_m
		F_u	u_u	W_u	$2W_{u,single}/W_{u,double}$	F_u/F_u	u_u/u_u	W_u/W_u	
[mm]	[%]	[N]	[mm]	[Nmm]	[-]	[-]	[-]	[-]	[-]
2	50	26	8.3	105		0.75	0.62	0.76	
2	80	41	14.5	372		0.75	0.14	0.14	
4	50	60	9.8	372		1.07	0.79	1.06	
4	80	77	7.0	294		1.31	0.45	0.86	
2 & 2	50			526	0.40				0.16
2 & 2	80			1092	0.68				0.47
4 & 4	50			1187	0.63				0.39
4 & 4	80			544	1.08				1.17

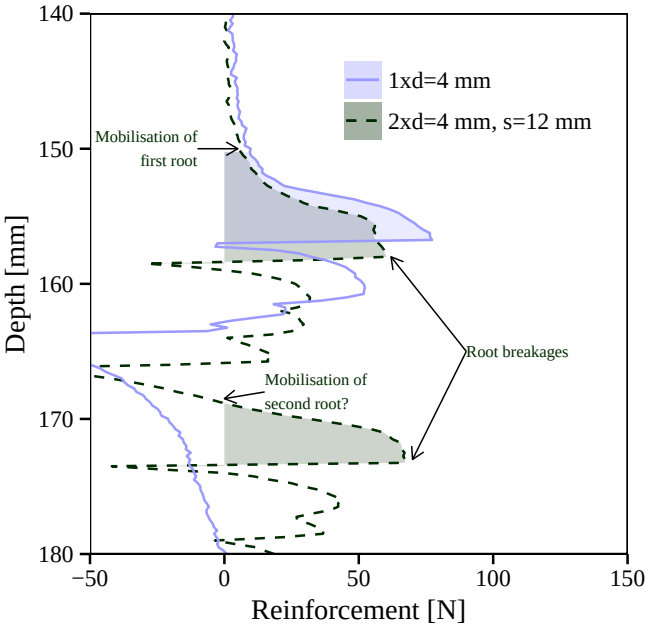

Figure 6: Root reinforcement traces for a single and two $d = 4$ mm roots in $I_d = 80\%$ sand. 's' is root centre-to-centre distance. Shaded areas indicate root action.

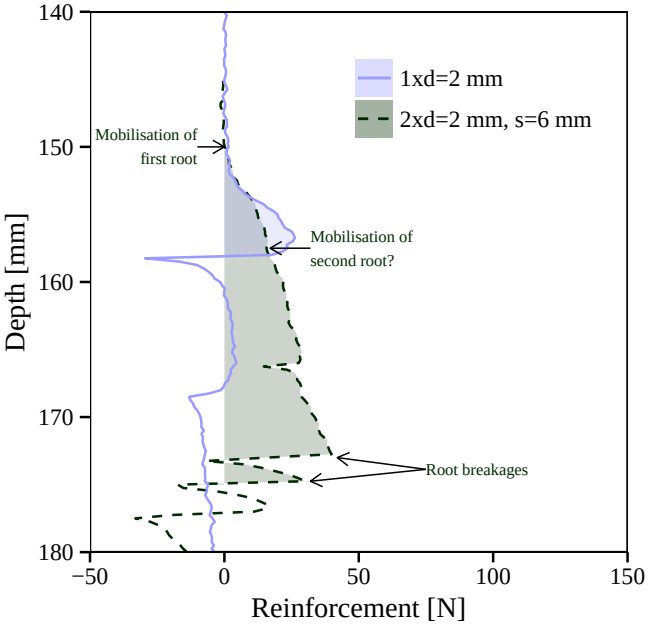

Figure 7: Root reinforcement traces for a single and two $d = 2$ mm roots in $I_d = 50\%$ sand. 's' is root centre-to-centre distance. Shaded areas indicate root action.

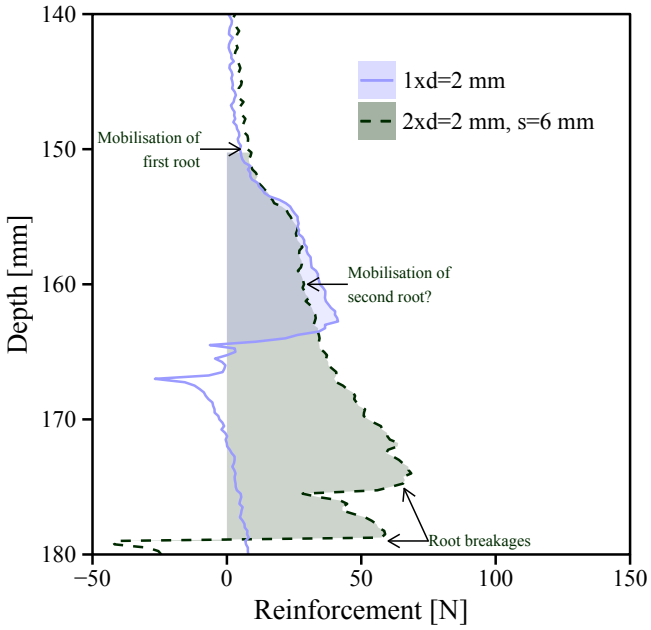

Figure 8: Root reinforcement traces for a single and two $d = 2$ mm roots in $I_d = 80\%$ sand. 's' is root centre-to-centre distance. Shaded areas indicate root action.

the increased amount of work dissipated by closely spaced roots. The same holds for the increase in lateral root displacement u_u. An explanation for this reduction in p_u can be found by looking into the mobilisation mechanism of the soil resistance. It is hypothesised p_u will reduce on the first load once the second root analogue is mobilised since the first root moves through a zone 'shaded' by the second root (Figure 9).

Such a reduction in p_u bears similarities to reductions in lateral pile capacity for piles in pile groups compared to single piles. This reduction can be taken into account by reducing the lateral resistance by a factor f_m, a so-called p-multiplier (e.g. Brown et al. 1988). McVay et al. (1995) conducted centrifuge tests on a 3×3 pile configurations in dry sand, spaced at $s/d = 3$. For loose sand ($I_d = 33\%$) they found $f_m = 0.65$, 0.45 and 0.35 for piles in the leading row, middle row and back row respectively. For medium dense sand ($I_d = 55\%$), these values were 0.8, 0.4 and 0.3 respectively. This shows that the more a pile is 'shielded' by piles ahead of it, the lower the lateral soil resistance will be, an effect that will be more pro-

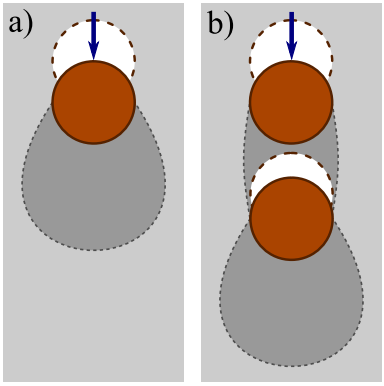

Figure 9: Schematic representation of mobilisation of soil resistance in the case of two roots.

nounced in looser soil.

To explain the amount of work dissipated in the testing described in this paper, average p-multipliers required are either higher ($d = 4$ mm, $I_d = 80\%$) or lower (all other tests) compared to these literature values (see Table 1, last column), despite similar s/d values as used by McVay et al. (1995). One explanation for the lower values is that literature values for f_m are typically derived from tests with relative small relative displacements between piles. In the case of McVay et al. (1995), piles were connected at the top to model a superstructure, resulting in s/d not significantly changing during the test. However, in the tests described here the first root hit will slowly move towards the second root. Therefore s/d will reduce with increasing penetrometer displacement before breakage, resulting in gradually decreasing values of f_m. This reduction might be smaller when the ratio between u_u and s is small since the root will have failed before the first root reaches the non-displaced position of the second root. This might (partially) explain why f_m values measured for the test in $I_d = 80\%$ using $d = 4$ mm root analogues were higher compared to the other tests.

5 CONCLUSIONS

It was shown that root–soil–root interaction has a significant effect on the behaviour of root analogues loaded by a blade penetrometer. Due to a reduction in soil resistance caused by close spacing, root analogues displaced further and dissipated more energy compared to tests only containing a single root. This effect was particularly pronounced for the first root hit. These effects will be stronger when the displacement required to failure is large compared to the root spacing (large u_u/s), for example in weaker soils or for strong, flexible roots. However, not enough test data was available to quantify the magnitude of the soil resistance reduction factor f_m (p-multiplier) as a function of soil properties, root properties and root spacing.

As a result of root–soil–root interaction, closely spaced roots will not necessarily appear as discrete separate peaks in the depth-penetrometer resistance trace. The experiments showed that they might break at a similar point in time. In these cases, inferring root properties from the amount of energy dissipated by displacing roots might be more feasible.

The existing penetrometer method is currently most suitable for identifying more widely spaced structural roots. Physical modelling indicated that development of an interpretative model should look at root-soil-root interaction when roots are closely spaced.

REFERENCES

Achat, D. L., M. R. Bakker, & P. Trichet (2008). Rooting patterns and fine root biomass of *Pinus pinaster* assessed by trench wall and core methods. *Journal of Forest Research 13*(3), 165–175.

Bischetti, G. B., E. A. Chiaradia, T. Simonato, B. Speziali, B. Vitali, P. Vullo, & A. Zocco (2005). Root strength and root area ratio of forest species in Lombardy (northern Italy). *Plant and Soil 278*(1–2), 11–22.

Brown, D. A., C. Morrison, & L. C. Reese (1988). Lateral load behaviour of pile groups in sand. *ASCE Journal of Geotechnical Engineering 114*(11), 1261–1276.

Coppin, N. & I. Richards (1990). *Use of vegetation in civil engineering, CIRIA book 10*. Kent: Butterworths.

Giadrossich, F., M. Schwarz, D. Cohen, F. Preti, & D. Or (2013). Mechanical interactions between neighbouring roots during pullout tests. *Plant and Soil 367*(1–2), 391–406.

Jackson, R. B., J. Canadell, J. R. Ehleringer, H. A. Mooney, O. E. Sala, & E. D. Schulze (1996). A global analysis of root distribution for terrestial biomes. *Oecologica 108*(3), 389–411.

Lauder, K. (2010). *The performance of pipeline ploughs*. Ph. D. thesis, University of Dundee.

Liang, T., J. Knappett, & N. Duckett (2015). Modelling the seismic performance of rooted slopes from individual root–soil interaction to global slope behaviour. *Géotechnique 65*(12), 995–1009.

McVay, M., R. Casper, & T.-I. Shang (1995). Lateral response of three-row groups in loose to dense ssand at 3d and 5d pile spacing. *ASCE Journal of Geotechnical Engineering 121*(5), 436–441.

Meijer, G. J. (2016). *New methods for in situ measurement of mechanical root-reinforcement on slopes*. Ph. D. thesis, University of Dundee.

Meijer, G. J., A. G. Bengough, J. A. Knappett, K. W. Loades, & B. C. Nicoll (2016). New in-site techniques for measuring the properties of root-reinforced soil – laboratory evaluation. *Géotechnique 66*(1), 27–40.

Meijer, G. J., A. G. Bengough, J. A. Knappett, K. W. Loades, & B. C. Nicoll (2017a). In situ root identification through blade penetrometer testing – part 1: interpretative models and laboratory testing. *Géotechnique*. Published ahead of print.

Meijer, G. J., A. G. Bengough, J. A. Knappett, K. W. Loades, & B. C. Nicoll (2017b). In situ root identification through blade penetrometer testing – part 2: field testing. *Géotechnique*. Published ahead of print.

Reese, L. C. & W. F. Van Impe (2011). *Single piles and pile groups under lateral loading, 2nd edition*. Leiden, The Netherlands: CRC.